Neuron, Vol. 20, 749–761, April, 1998, Copyright ©1998 by Cell Press

Olfactory Reciprocal Synapses: Dendritic Signaling in the CNS

Jeffry S. Isaacson* and Ben W. Strowbridge*†‡
*Department of Physiology and Biophysics
†Department of Neurological Surgery
University of Washington
Seattle, Washington 98195

Summary

Synaptic transmission between dendrites in the olfactory bulb is thought to play a major role in the processing of olfactory information. Glutamate released from mitral cell dendrites excites the dendrites of granule cells, which in turn mediate GABAergic dendrodendritic inhibition back onto mitral dendrites. We examined the mechanisms governing reciprocal dendritic transmission in rat olfactory bulb slices. We find that NMDA receptors play a critical role in this dendrodendritic inhibition. As with axonic synapses, the dendritic release of fast neurotransmitters relies on N- and P/Q-type calcium channels. The magnitude of dendrodendritic transmission is directly proportional to dendritic calcium influx. Furthermore, recordings from pairs of mitral cells show that dendrodendritic synapses can mediate lateral inhibition independently of axonal action potentials.

Introduction

Fast synaptic transmission in the brain is typically mediated by neurotransmitters released from axon nerve endings. However, a prominent role for dendritic transmitter release has been suggested in several regions of the CNS, such as the substantia nigra (Cheramy et al., 1981) and retina (Dowling, 1968). While much attention has been focused on the mechanisms underlying transmitter release from conventional axon terminals, relatively little is known about factors governing dendritic transmitter release. To investigate such mechanisms, we studied the mammalian olfactory bulb where reciprocal dendrodendritic synapses play a central role in odor detection (Yokoi et al., 1995).

The olfactory bulb is the first site for the processing of olfactory information in the mammalian brain (Shepherd and Greer, 1990). Mitral cells are the principal neurons of the olfactory bulb and send excitatory projections to the piriform cortex (Figure 1A). Mitral cells have a highly specialized structure. They receive excitatory input from olfactory nerve fibers via conventional axonic nerve terminals on the distal tufts of their primary dendrites. Mitral cells also receive a large number of inhibitory synaptic contacts primarily on their lateral (secondary) dendrites, which extend for large distances across the olfactory bulb. These inhibitory contacts arise from the large spines of axonless local interneurons, the granule cells. Electron microscopic evidence indicates that mitral cell dendrites contain synaptic vesicles clustered around active zones (Rall et al., 1966; Price and Powell, 1970a, 1970b). Granule cells contact mitral cells via large, vesicle-containing spines that are both pre- and postsynaptic to mitral cell dendrites. Virtually all of these contacts directly oppose mitral cell release sites, and this synaptic arrangement is believed to form the basis for reciprocal dendrodendritic inhibition of mitral cells (Rall et al., 1966; Rall and Shepherd, 1968).

The basic physiological properties of this dendrodendritic circuit were described initially in the rabbit olfactory bulb (Phillips et al., 1963; Nicoll, 1969) and subsequently confirmed in the turtle (Jahr and Nicoll, 1980, 1982a, 1982b; Nowycky et al., 1981) and salamander (Wellis and Kauer, 1993, 1994). These studies demonstrated an important role for $GABA_A$ receptors in the reciprocal inhibition of mitral cells. It has been proposed that glutamate released from mitral cell dendrites excites granule cell spines (Jahr and Nicoll, 1982b; Wellis and Kauer, 1993, 1994); however, the postsynaptic receptors that drive GABA release in mammalian granule cell dendrites are not well defined. Throughout the CNS, non-NMDA (N-methyl-D-aspartate) glutamate receptors mediate the majority of fast excitatory transmission, whereas NMDA receptors are thought to play a critical role in synaptic plasticity and development (Collingridge and Lester, 1989). However, the high level of expression of NMDA receptors in granule cell dendrites (Cotman and Iverson, 1987) raises the possibility that these receptors play a central role in olfactory processing.

The reciprocal dendrodendritic circuit provides a reliable mechanism for spatially localized self-inhibition of mitral cells. In addition, the extensive lateral dendrites of mitral cells and the convergence of inputs from multiple mitral cells onto single granules are thought to provide the basis of lateral inhibition and odor discrimination (Yokoi et al., 1995; Brennan and Keverne, 1997).

The olfactory bulb, therefore, relies on both conventional axonic synaptic transmission as well as local release of fast neurotransmitters from dendrites. It is unclear whether common mechanisms regulate transmitter release from both dendrites and axons, since the calcium channels and intracellular calcium dynamics that underlie dendrodendritic inhibition are unknown. To address these questions, we have explored the mechanisms governing dendrodendritic inhibition in slices of the rat olfactory bulb. Using patch-clamp recording from mitral and granule cells, we find that both NMDA and non-NMDA receptors are critical for the generation of dendrodendritic inhibition. Our results also indicate that high voltage–activated calcium channels of the N and P/Q class play a dominant role in dendritic transmission. Studies of neurons in several different cortical brain regions have revealed active properties of neuronal dendrites (Johnston et al., 1996; Stuart et al., 1997). We have used photometric measurements of calcium signals to test for active properties in mitral cell dendrites. To study the relationship between mitral cell activity and the generation of the dendrodendritic response, we have made

‡Present address: Department of Neuroscience, Case Western Reserve University, Cleveland, Ohio 44118.

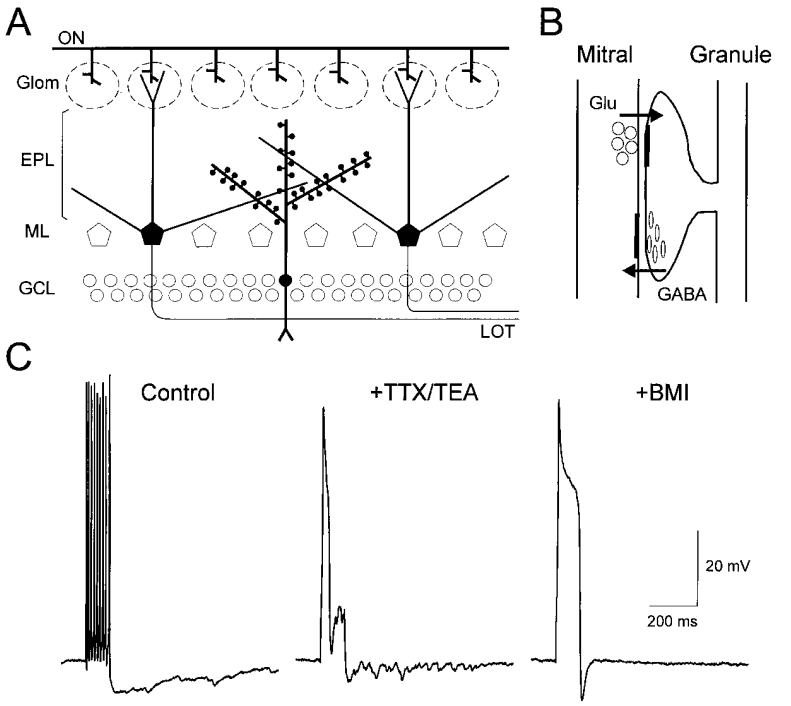

Figure 1. Dendrodendritic Inhibition in the Rat Olfactory Bulb Slice

(A) Schematic of the olfactory bulb slice. ON, olfactory nerve; Glom, glomerular layer; EPL, external plexiform layer; ML, mitral cell layer; GCL, granule cell layer; LOT, lateral olfactory tract.

(B) Schematic of the reciprocal synaptic arrangement between the dendrites of mitral and granule cells.

(C) Current-clamp recording of dendrodendritic inhibition in a mitral cell. A depolarizing current step (0.3 nA, 100 ms) evokes a train of action potentials followed by a slow afterhyperpolarization (Control). The afterhyperpolarization persists in the presence of TTX and TEA. The response is abolished following the addition of bicuculline (+BMI).

simultaneous recordings of dendritic calcium influx and dendrodendritic inhibition. The extent of reciprocal inhibition was closely related to the magnitude of calcium influx in the mitral cell dendrite. Using dual recordings from neighboring mitral cells, we also studied the propagation of dendritic signals between principal cells. We show that dendrodendritic synapses can mediate lateral inhibition in a manner that does not require voltage-gated sodium channels.

Results

We first tested for the presence of dendrodendritic feedback inhibition in mitral cells using current-clamp recordings in slices of the rat olfactory bulb. Depolarizing current steps evoked a train of action potentials in mitral neurons that was followed by a long-lasting afterhyperpolarization (Figure 1C). Following the application of tetrodotoxin (TTX, 1 μM) to block sodium-dependent action potentials and tetraethylammonium (TEA, 5 mM) to block potassium channels, current steps evoked a calcium spike followed by an afterhyperpolarization, similar to that seen under control conditions. The long-lasting afterhyperpolarization appeared to be composed of the summation of individual inhibitory postsynaptic potentials (IPSPs). The subsequent addition of the $GABA_A$ receptor antagonist bicuculline methiodide (BMI, 10–20 μM) abolished the afterhyperpolarization, confirming that the response was mediated by $GABA_A$ receptors. These results suggest that this feedback inhibition of mitral cells was mediated by dendritic interactions since the response persisted in TTX, which blocks all axonal conduction. The simplest interpretation of these results is that mitral cell dendrites release an excitatory transmitter, presumably glutamate, which excites granule cell spines and leads to the release of GABA back onto the mitral cell (Figure 1B). These results demonstrate that dendrodendritic inhibition is preserved in the rat olfactory bulb slice.

We next examined dendrodendritic inhibition in voltage-clamp recordings from mitral cells. The whole-cell recording pipette contained a CsCl-based internal solution, which sets the reversal potential for $GABA_A$ receptor–mediated responses near 0 mV; inhibitory postsynaptic currents (IPSCs) should then be inward currents at negative holding potentials. To evoke dendrodendritic inhibition, we applied a brief (10 ms) depolarizing step from −70 to 0 mV. Under control conditions, this step generated a large action current composed primarily of sodium channel–mediated current. The action current was followed by a slow inward current that was apparently generated by the summation of many individual IPSCs (Figure 2A). Following the addition of TTX, the fast action current was blocked, and when the depolarizing voltage step was lengthened, a large inward calcium current was evoked. In the presence of TTX, the calcium current was followed by a slowly decaying barrage of IPSCs that was similar to the response generated under control conditions (Figure 2A). These results demonstrate that inhibitory synaptic currents in mitral cells can be elicited through purely dendritic interactions. Unless otherwise indicated, all following experiments were performed in the presence of TTX. To illustrate the synaptic component of evoked responses more clearly, we blanked the calcium current generated during the voltage step. Under these conditions, the slow evoked responses (peak amplitude = 1.2 ± 0.3 nA) decayed with a time constant of 513 ± 58 ms (n = 8) and were abolished by BMI (n = 6; Figure 2B). The evoked response also was blocked completely by the inorganic calcium channel antagonist, cadmium (100 μM, n = 6; Figure 2C). These results establish that the evoked IPSC is mediated by

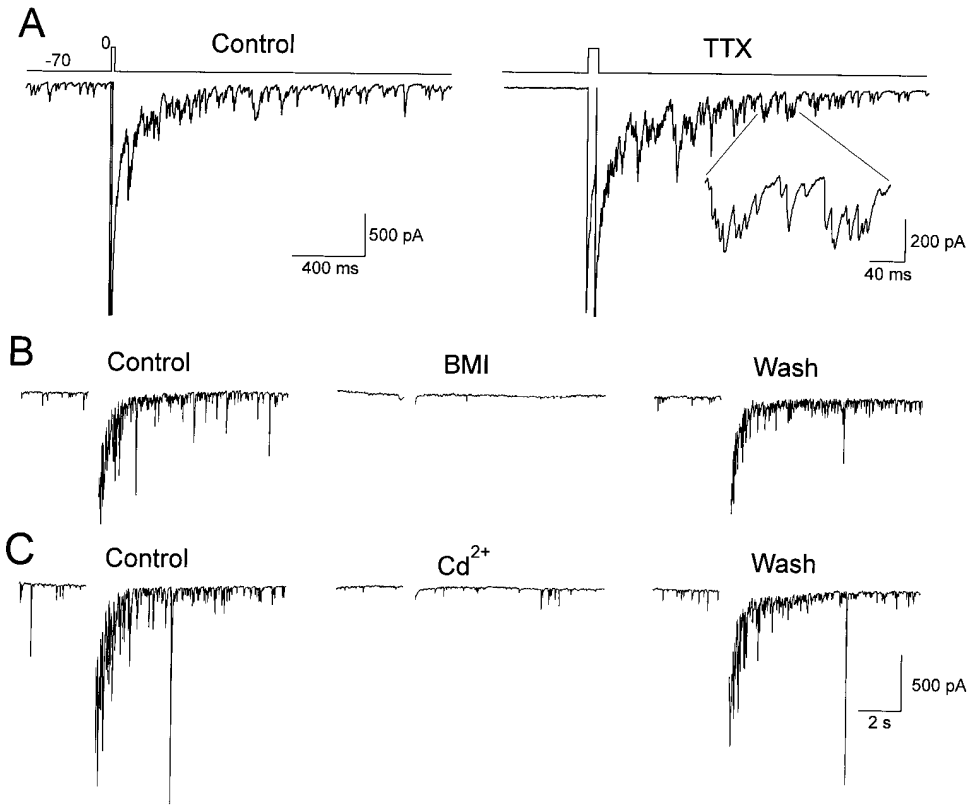

Figure 2. Voltage-Clamp Recordings of Dendrodendritic Inhibition

(A) Brief (10 ms) voltage steps evoke an action current (clipped) followed by a slow synaptic current (Control). Similar synaptic response currents can be evoked following slightly longer voltage steps (50 ms), which generate large calcium currents in TTX. These long-lasting synaptic responses reflect dendrodendritic inhibition of mitral cells and are composed of the summation of many discrete IPSCs (inset).

(B) Dendrodendritic inhibition is blocked by bicuculline (BMI, 10 μM).

(C) Dendrodendritic inhibition also is abolished by cadmium (Cd^{2+}, 100 μM).

$GABA_A$ receptors and that dendrodendritic inhibition requires voltage-gated calcium channels.

The majority of fast excitatory transmission in the brain is mediated by non-NMDA glutamate receptors (Collingridge and Lester, 1989). NMDA receptors, which have relatively slow kinetics and are highly permeable to Ca^{2+}, are generally thought to contribute little to transmission under resting conditions due to their voltage-dependent block by extracellular Mg^{2+}. We next sought to determine which subtypes of glutamate receptors on granule cell spines trigger the release of GABA. To quantitate dendrodendritic inhibition, we measured the integral of the current response following the voltage step. The non-NMDA receptor antagonist DNQX (6,7-dinitroquinoxaline-2,3-dione, 10–20 μM) caused a marked reduction in dendrodendritic inhibition evoked in all mitral cells examined (21.2% ± 6.2% of control, n = 9; Figure 3A). Surprisingly, the NMDA receptor antagonist APV (D-2-amino-5-phosphopentanoic acid, 25–50 μM) caused a similar marked reduction in the dendrodendritic response (19.6% ± 3.3% of control, n = 7; Figure 3B). The dendrodendritic response was virtually eliminated when both APV and DNQX were coapplied (7.0% ± 3.0% of control, n = 3). These results suggested that both NMDA and non-NMDA receptors are critical for the generation of GABA release from granule cell spines.

Why does dendrodendritic inhibition require both NMDA and non-NMDA glutamate receptors? One possibility we considered was that NMDA receptors were important for generating the response. If the two glutamate receptor types were colocalized on individual granule cell spines, depolarization driven by the non-NMDA receptors would be required to relieve the voltage-dependent Mg^{2+} block of the NMDA receptors. If this were the case, then dendrodendritic inhibition would be greatly enhanced in Mg^{2+}-free Ringer's solution. Indeed, we found a dramatic increase in the magnitude of dendrodendritic inhibition after washout of extracellular Mg^{2+} (peak amplitude = 2.4 ± 0.6 nA, n = 9; Figure $3B_1$). The decay time course of dendrodendritic inhibition evoked in Mg^{2+}-free solution (551 ± 40 ms, n = 9) was similar to that in control conditions. In Mg^{2+}-free solution, we found that dendrodendritic inhibition could be evoked by very brief (1–2 ms) voltage steps to the mitral cell. These responses were graded with the amount of calcium influx into the mitral cell (n = 6; Figure $3B_2$).

If dendrodendritic inhibition was generated preferentially by NMDA receptors, then it would be expected that the requirement for non-NMDA receptors would be greatly reduced in Mg^{2+}-free solution. Indeed, we found that while APV caused a marked reduction in dendrodendritic inhibition in Mg^{2+}-free solution (8.7% ± 1.9%

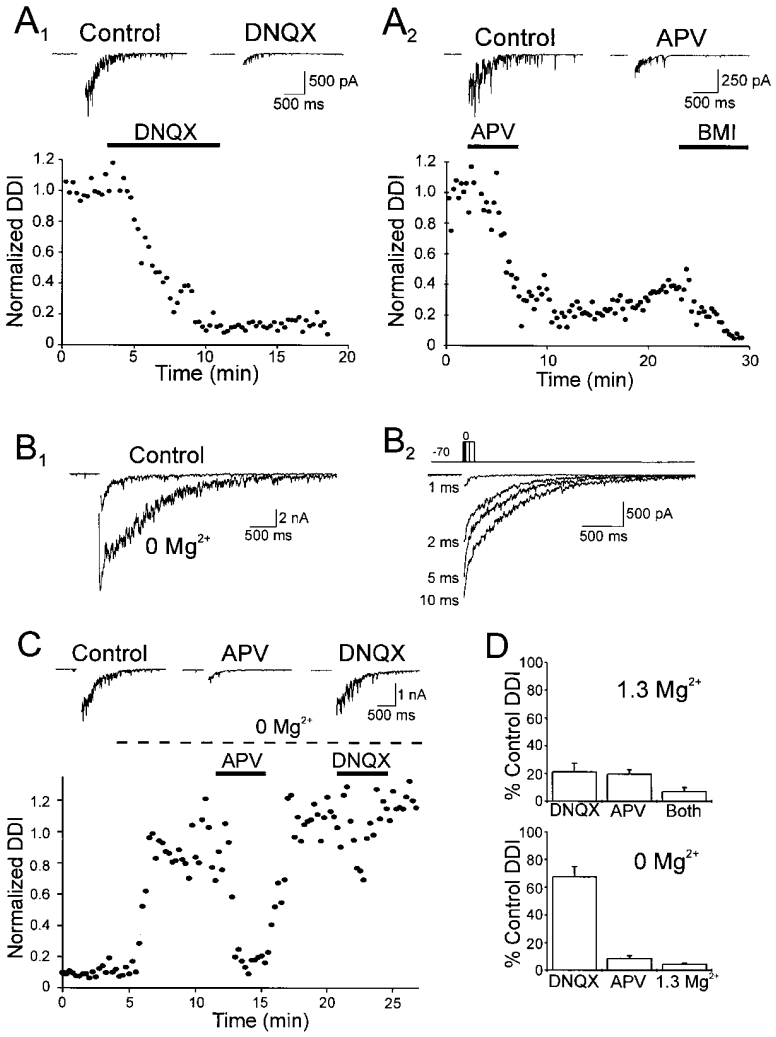

Figure 3. Importance of NMDA Receptors in Dendrodendritic Inhibition

(A_1) Plot of the reduction of dendrodendritic inhibition by the non-NMDA receptor antagonist DNQX (20 μM). Sample records from this mitral cell show dendrodendritic responses before (Control) and after the addition of DNQX.

(A_2) In another mitral cell, the NMDA receptor antagonist APV (25 μM) reduces dendrodendritic inhibition to a similar extent. The entire response remaining after partial washout of APV was abolished by BMI.

(B_1) Removing Mg^{2+} from the superfusing solution causes a dramatic enhancement of dendrodendritic inhibition in response to the same voltage step.

(B_2) Dendrodendritic inhibition in Mg^{2+}-free solution is graded with calcium influx into the mitral cell when evoked by voltage steps of varying durations.

(C) In Mg^{2+}-free solution, dendrodendritic inhibition is governed almost entirely by NMDA receptors, while the role of non-NMDA receptors is reduced. The plot shows the results from one experiment. Mg^{2+}-free solution was substituted for the normal Ringer's solution during the period marked by the dashed line. Under these conditions, APV (25 μM) caused a marked reduction in dendrodendritic inhibition, but the subsequent application of DNQX (20 μM) had little effect. Sample sweeps show responses after washout of Mg^{2+} (Control), during the application of APV, and in the presence of DNQX.

(D) Summary of the actions of APV and DNQX in normal and Mg^{2+}-free Ringer solution.

of control, n = 13), DNQX was much less effective (67.5% ± 7.3% of control, n = 9; Figure 3C). Furthermore, restoring Mg^{2+} (1.3 mM) to this solution blocked dendrodendritic inhibition (4.5% ± 0.7% of control, n = 6) to an extent similar to APV. The results from experiments in normal and Mg^{2+}-free solution are summarized in Figure 3D. Taken together, these results demonstrate that NMDA receptors play a dominant role in triggering the release of GABA from granule cell spines.

Since both NMDA and non-NMDA receptors are involved in dendrodendritic inhibition, we next studied directly the glutamate receptors that mediate excitatory transmission onto granule cell spines. We recorded from granule cells in the absence of TTX and used a focal stimulating electrode to evoke glutamate release from the dendrites of nearby mitral cells (Figure 4A). Stimulation in the external plexiform layer (EPL) evoked excitatory postsynaptic currents (EPSCs) in granule cells in the presence of BMI. At −80 mV, EPSCs decayed with a rapid time course. In all cells examined (n = 5), membrane depolarization revealed a slow component to the decay of the evoked EPSC (Figure 4A). The slow component was blocked by APV and the remaining fast component was abolished by DNQX (n = 3). These results indicate that excitatory transmission between mitral and granule cells is mediated by both NMDA and non-NMDA receptors. Furthermore, these findings are consistent with the involvement of both glutamate receptor subtypes in dendrodendritic inhibition.

We then asked whether calcium channels in granule cell spines were coupled directly to the release of GABA. To address this question, we recorded from mitral cells and depolarized granule cell dendrites using focal application of 90 mM KCl in the presence of TTX (Figure 4B). Local depolarization of the granule cell dendrites was alternated with voltage pulses to a mitral cell to monitor dendrodendritic inhibition. Brief (100 ms) applications of KCl into the EPL evoked a barrage of IPSCs that resembled the response generated by voltage steps to the mitral cell (Figure 4B). The coapplication of DNQX and APV completely blocked the dendrodendritic inhibition evoked from voltage steps to the mitral cell; however, the response to KCl was maintained. The simplest interpretation of these findings is that KCl directly depolarized granule cell spines leading to the release of GABA. The subsequent addition of cadmium (100 μM) abolished this response. Similar results were obtained

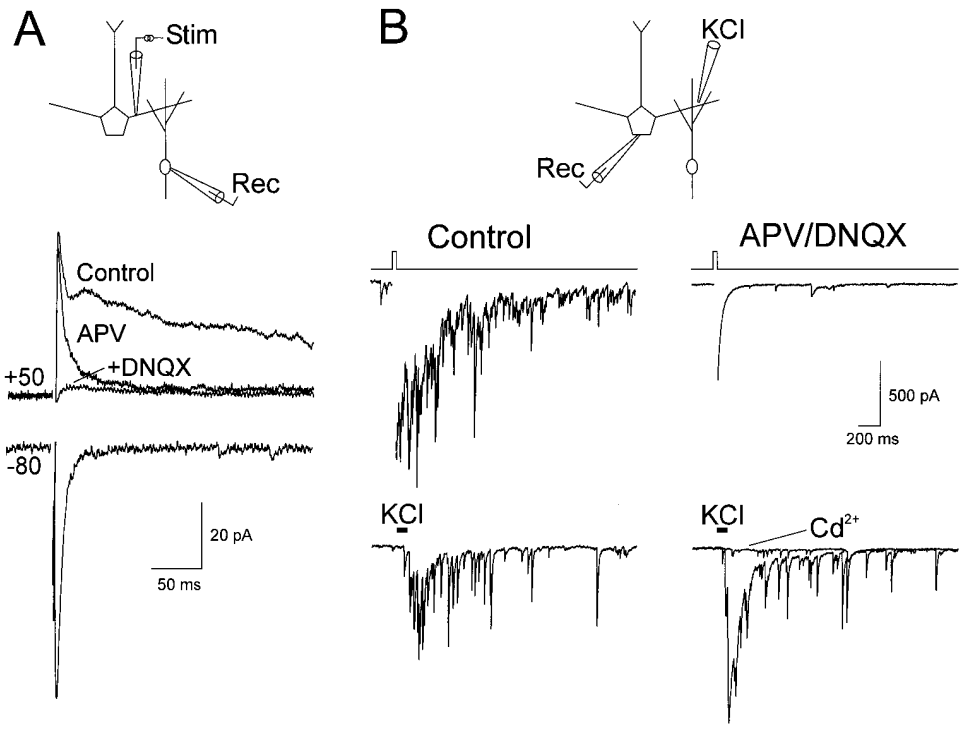

Figure 4. Synaptic Properties of Granule Cells

(A) Both NMDA and non-NMDA receptors mediate excitatory transmission in granule cells. EPSCs recorded from a granule cell were evoked by extracellular stimulation of mitral cell dendrites (schematic). At −80 mV, a fast EPSC is evoked in granule cells. Depolarization of the granule cell to −50 mV reveals a slow component of the EPSC. The slow component is blocked by APV (25 μM) and the remaining fast component is abolished by DNQX (20 μM).

(B) Calcium channels in granule cell spines trigger GABA release. IPSCs recorded from a mitral cell in response to brief applications of 90 mM KCl from a puffer pipette (100 ms, 10 lb/in^2) placed within the EPL (see schematic). Application of KCl (bar) in the presence of TTX (1 μM) evokes a synaptic response (lower traces) that is similar to the dendrodendritic inhibition elicited in the same cell following a voltage step (upper traces). Following the coapplication of APV (25 μM) and DNQX (20 μM), dendrodendritic inhibition is abolished but the response to KCl is undiminished. The subsequent addition of cadmium (100 μM) completely abolishes the response evoked by focal depolarization.

in two other cells. These findings provide strong evidence that entry of calcium through voltage-dependent calcium channels in granule cell spines is sufficient to trigger GABA release onto mitral cell dendrites.

The release of glutamate from conventional axonic synapses requires strong depolarization to open high threshold calcium channels that control exocytosis (Dunlap et al., 1995). If a similar mechanism governs the release of transmitter in the olfactory bulb, glutamate release may depend upon the propagation of large-amplitude action potentials through dendrites to activate local calcium channels. We used several approaches to address the active properties of mitral dendrites. We first made simultaneous recordings from the soma and dendrites of individual mitral cells to establish the dendritic propagation of action potentials in these neurons (Figure 5A). Dual current-clamp recordings were made from the soma and at locations up to 250 μm away (average distance 155 ± 19 μm) on primary dendrites using a K^+-based internal solution in the absence of TTX. Action potentials were evoked by small depolarizing current steps applied at the somatic or dendritic recording site. In all cases (n = 7), the amplitudes of action potentials recorded at the dendritic location (84 ± 7 mV) were similar to those recorded at the soma (87 ± 4 mV). Furthermore, action potentials always initiated first at the somatic site, regardless of the site of current injection (Figure 5A). These results indicate that action potentials initiated close to the soma of mitral cells and back-propagated through dendrites with little decrement.

Another requirement for the dendritic release of glutamate is the activation of calcium channels in mitral cell dendrites following action potential invasion. To examine this possibility, we measured the calcium transients evoked by single action potentials in mitral cells filled with the fluorescent calcium indicator Oregon Green (100 μM). A photodiode was used to monitor the change in fluorescence (ΔF/F) at several locations in the same mitral cell following single action potentials (Figure 5B). Action potentials triggered calcium transients in the soma, primary and secondary dendrites, as well as the distal dendritic tuft of mitral cells (Figure 5B$_1$). These results indicate that single action potentials lead to calcium influx in the dendrites of mitral cells that is presumably mediated by calcium channels. To confirm the presence of calcium channels in the dendrites, we examined the effects of nickel and cadmium on the action potential-evoked calcium transients. Low concentrations of

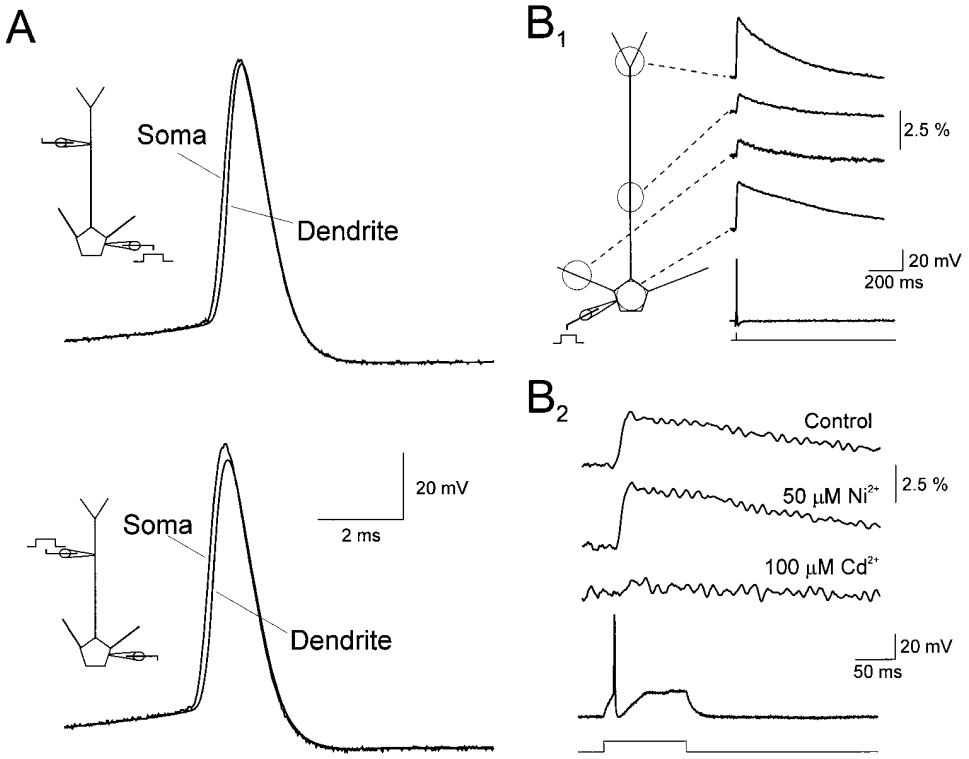

Figure 5. Action Potentials Propagate into the Dendrites of Mitral Cells and Activate Dendritic Calcium Channels

(A) Simultaneous recording of action potentials at the soma and dendrite (150 μm from the somatic electrode). Upper traces show action potentials evoked by a depolarizing current pulse injected at the soma (0.2 nA). Lower traces are from the same cell showing the responses evoked when the depolarizing step was delivered to the dendritic electrode. In both cases, the action potential occurs first at the somatic location.

(B_1) Single action potentials evoke calcium influx in mitral cell dendrites. Calcium transients were measured at the regions indicated by the circles in response to action potentials evoked at the soma by depolarizing current injection (lower sweeps).

(B_2) Calcium transients recorded in the secondary dendrites of a mitral cell in response to single action potentials (lower sweeps) are insensitive to nickel (50 μM) but are abolished by cadmium (100 μM).

nickel (50 μM) had no effect on calcium influx, whereas cadmium (100 μM) completely blocked the response (Figure 5C). Similar results were obtained in three mitral cell recordings. Since low voltage–activated (T-type) calcium channels are generally sensitive to nickel (Avery and Johnston, 1996), these results suggest that only high threshold calcium channels mediate dendritic calcium influx following single action potentials.

We next asked whether the calcium channels that regulate glutamate release from mitral cell dendrites were near or far from vesicle release sites. To address this question, we studied the effects of the calcium chelators 1,2-bis(2-aminophenoxy)ethane-N,N,N′,N′-tetraacetic acid (BAPTA) and ethylene glycol-bis(β-aminoethyl ether)-N,N,N′,N′-tetraacetic acid (EGTA) on dendrodendritic inhibition. In most axonal presynaptic terminals studied previously, only chelators that have very rapid calcium binding kinetics (e.g., BAPTA) can completely suppress neurotransmitter release (Adler et al., 1991). By contrast, chelators with similar affinities for calcium, but relatively slow binding kinetics (e.g., EGTA), have little or no effect on single evoked synaptic responses. These findings have been used to suggest that calcium channels must be very close to the sites of vesicle exocytosis, since only chelators with very rapid kinetics are able to intercept calcium ions before they trigger transmitter release. It is not known whether similarly tight coupling between voltage-gated calcium channels and vesicle release machinery exists in the presynaptic dendrites of the olfactory bulb.

Mitral cells were recorded with our standard internal solution (containing 0.2 mM EGTA) or alternately with ones containing 20 mM BAPTA or 20 mM EGTA. Dendrodendritic inhibition was measured from the time of patch rupture at the start of whole-cell recording. Under control conditions, the dendrodendritic responses gradually increased in magnitude during the first 3 min of whole-cell recording (Figure $6A_1$), presumably due to the loading of the mitral cells with both cesium and chloride. Results were normalized to the steady-state responses of the control mitral cells. In mitral cells recorded with BAPTA, dendrodendritic responses to single voltage steps were virtually absent (4% of control, $n = 6$; Figures $6A_1$ and $6A_2$). Dendrodendritic transmission could be restored in BAPTA-loaded cells by applying short trains of voltage steps (Figure $6A_3$), suggesting that the summation of three to five BAPTA-attenuated calcium transients was sufficient to trigger glutamate release. The ability to overcome the blocking actions of BAPTA with repetitive stimulation has been described previously at

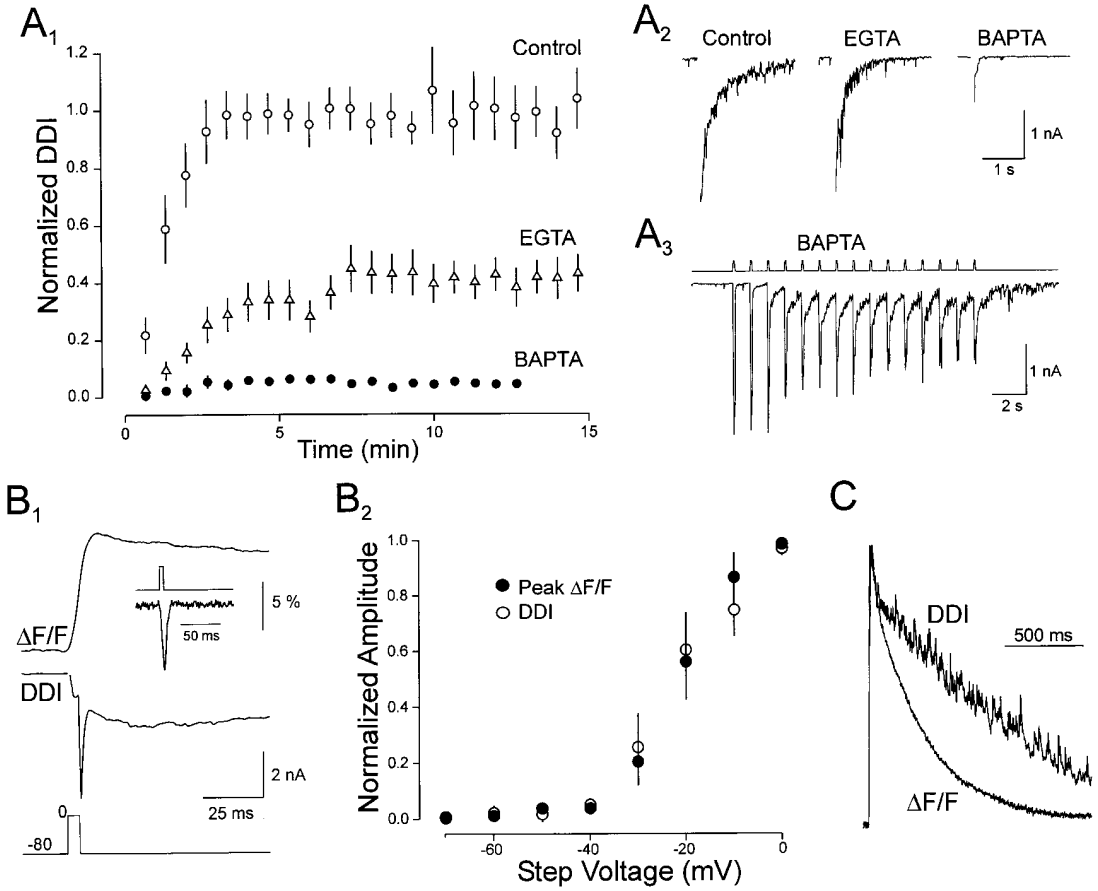

Figure 6. Relationship between Mitral Dendrite Calcium Influx and Dendrodendritic Inhibition

(A_1) Summary plot of the effect of loading mitral cells with EGTA (triangles) or BAPTA (closed circles). Records are normalized with respect to the steady-state response recorded under control conditions (0.2 mM EGTA, open circles).

(A_2) Representative dendrodendritic inhibition from cells recorded with 0.2 mM EGTA (control), 20 mM EGTA, and 20 mM BAPTA.

(A_3) Although the response to single voltage steps is abolished in BAPTA-loaded cells, a train of voltage steps restores dendrodendritic inhibition. Calcium current during the voltage step has not been blanked in this recording (same cell as shown above, BAPTA).

(B_1) Simultaneous recording of dendrodendritic inhibition (DDI) and calcium influx ($\Delta F/F$) in the secondary dendrite of a mitral cell. Calcium current has not been blanked from the current trace. The first derivative of the calcium transient, indicating the time course of calcium influx, activates rapidly and ends shortly after the voltage step (inset).

(B_2) Summary of the relationship between dendrodendritic inhibition (open circles) and dendritic calcium influx (closed circles) in seven cells. Calcium influx was changed by altering the amplitude of the voltage steps (5 ms duration) applied to mitral cells. Responses are normalized to the values obtained with a voltage step to 0 mV. Both dendrodendritic inhibition and mitral dendrite calcium influx activate at approximately −30 mV.

(C) Comparison of the time course of dendrodendritic inhibition and calcium clearance from mitral dendrites. The current response to a voltage step has been inverted and scaled to match the peak amplitude of the calcium transient recorded in the secondary dendrite of the same cell. All experiments were performed in Mg^{2+}-free solution.

the crayfish neuromuscular junction (Winslow et al., 1994) and giant synaptic terminals of bipolar neurons (von Gersdorff and Matthews, 1994). In marked contrast to BAPTA, all mitral cells loaded with a similar concentration of EGTA demonstrated reliable but diminished dendrodendritic inhibition (44% of control, n = 9) in response to single voltage steps. The clear difference between the ability of BAPTA and EGTA to suppress dendrodendritic inhibition suggests that the calcium channels triggering glutamate release are located in relatively close proximity to the proteins governing exocytosis.

We next made simultaneous recordings of dendrodendritic inhibition and mitral dendrite calcium influx to explore further the relationship between dendritic calcium and transmitter release from mitral cells. In these experiments, our standard CsCl-based internal solution was supplemented with the low affinity calcium indicator Oregon Green-5N (100 μM). A typical example of dendrodendritic inhibition and the corresponding calcium transient measured in a mitral cell secondary dendrite are shown in Figure $6B_1$. In this case, the current response during the voltage step has not been blanked, and an inward calcium current during the voltage step as well as a larger calcium tail current can be seen. The first derivative of the fluorescence transient (Figure $6B_1$, inset), corresponding to the time course of calcium influx into the dendrite, activates during the voltage step and

decays rapidly following the end of the step. The rapid time course of photometrically measured calcium influx indicates that we have good voltage control of the secondary dendrites in these recordings. The rapid kinetics of calcium influx and its close correspondence to the time course of the measured calcium current also suggest that calcium-induced calcium release does not contribute significantly to glutamate release from mitral cell dendrites. We next examined the relationship between calcium influx and dendrodendritic inhibition by varying the amplitude of the voltage step applied to the mitral cell. Both calcium influx and dendrodendritic inhibition began to activate at −30 mV and were maximal at 0 mV, confirming the importance of high voltage–activated calcium channels in the release of glutamate (Figure 6B$_2$; n = 7 cells). When both dendrodendritic inhibition and calcium influx were normalized, we found that the activation of dendrodendritic inhibition paralleled closely the amount of calcium influx in mitral cell secondary dendrites.

What underlies the slow time course of dendrodendritic inhibition? We examined the relationship between the time course of dendrodendritic inhibition and calcium clearance from the mitral dendrites. We considered the possibility that the time course of dendrodendritic inhibition followed calcium dynamics in mitral dendrites. However, the decay time constant of the calcium signal was 4.0 ± 0.4–fold faster than the decay of dendrodendritic inhibition (n = 3). These results imply that the clearance of calcium from mitral dendrites is not the rate-limiting step governing the time course of dendrodendritic inhibition. However, the decay kinetics of dendrodendritic inhibition were temperature dependent (Q_{10} = 2.3 ± 0.7, n = 3), suggesting that active processes shape the time course of these responses. This temperature dependence also rules out the possibility that diffusion of glutamate underlies the time course of dendrodendritic inhibition.

Immunolocalization and electrophysiological studies indicate that a variety of calcium channel subtypes are present on the dendrites of central neurons (Westenbroek et al., 1990, 1992; Magee and Johnston, 1995). What are the relevant calcium channels underlying dendrodendritic inhibition? We explored this question by examining the action of several pharmacological blockers that discriminate between the various classes of identified calcium channels. The dihydropyridine nifedipine (10–20 μM) had no effect on dendrodendritic inhibition (103% ± 8% of control, n = 5; Figure 7A). This rules out the involvement of L-type calcium channels at either the mitral cell dendrite or granule spine release sites. Although nickel is nonspecific at high concentrations, at low concentrations nickel blocks T- and R-type channels (Avery and Johnston, 1996; Randall and Tsien, 1997). At a concentration of 50 μM, nickel caused only a slight reduction in dendrodendritic inhibition (84% ± 8% of control, n = 6; Figure 7A). Apparently, neither the T nor the R classes of channels play an important role in dendrodendritic transmission.

At conventional axonic synapses in several brain regions, glutamate and GABA release are thought to rely on N- or P/Q-type calcium channels (Takahashi and Momiyama, 1993; Castillo et al., 1994; Wheeler et al., 1994; Poncer et al., 1997). It has also been suggested at several synapses that both channel types can contribute to transmitter release from single nerve endings (Castillo et al., 1994; Mintz et al., 1995). We next examined the involvement of these channels by studying the effects of the ω-conotoxins GVIA and MVIIC. To confirm that the peptides were reaching the dendritic synapses at effective concentrations, we measured the field EPSP generated by conventional axonic nerve terminals of olfactory nerve (ON) fibers, which synapse on the distal dendritic tufts of mitral cells in the glomerular layer. An extracellular stimulating electrode was placed within bundles of the olfactory nerve, and an extracellular recording electrode was placed within a single glomerulus (Figure 7B; Aroniodou-Anderjaska et al., 1997). Stimulation of the ON inputs evoked a field EPSP that was blocked by a combination of DNQX and APV (Figure 7B). We monitored dendrodendritic inhibition and the field EPSP in slices superfused with Mg^{2+}-free solution in the absence of TTX. In these experiments, QX-314 (5 mM) was included in the mitral cell internal solution to remove the possibility that axon collaterals of mitral cells might contribute to the voltage step response. Application of ω-conotoxin GVIA (1 μM) caused a marked reduction in the ON field EPSP (44% ± 7% of control, n = 6). In the same slices, dendrodendritic inhibition was reduced to a lesser extent (67% ± 5% of control). Increasing the concentration of ω-conotoxin GVIA to 3 μM did not cause a further reduction in either the ON field EPSP nor dendrodendritic inhibition (n = 2). We next examined the actions of ω-conotoxin MVIIC (5 μM), which at high concentrations blocks P/Q- as well as N-type channels. Addition of ω-conotoxin MVIIC abolished the ON field EPSP (4% ± 2% of control, n = 6) and caused a dramatic reduction in dendrodendritic inhibition (27% ± 6% of control). Taken together, these results suggest that dendrodendritic inhibition depends on the P/Q class of calcium channels with a smaller role played by N-type channels. Both N- and P/Q-type channels govern transmission at the excitatory synapses formed by olfactory nerve fibers in the glomerular layer.

The secondary dendrites of mitral cells can extend across large regions of the olfactory bulb. The influence of a single mitral cell can be extended further, since single granule cells contact multiple mitral cells. This anatomical arrangement has been suggested to form the basis for lateral inhibition within the olfactory bulb, which is thought to represent an important mechanism for odor discrimination (Yokoi et al., 1995; Brennan and Keverne, 1997). We sought to determine whether dendrodendritic interactions could mediate lateral inhibition in the absence of sodium-dependent action potentials. One simple test for lateral inhibition is to record simultaneously from two mitral cells and to determine if dendritic glutamate release, evoked from one mitral cell by a voltage step, can elicit GABA release onto a second, unstimulated mitral cell. An example of this form of lateral inhibition in the presence of TTX is shown in Figure 8. A depolarizing voltage step to the first mitral cell (Cell 1) caused dendrodendritic self-inhibition and also evoked an IPSC in a nearby mitral cell (Cell 2). The IPSCs in both mitral cells were time-locked to the depolarizing

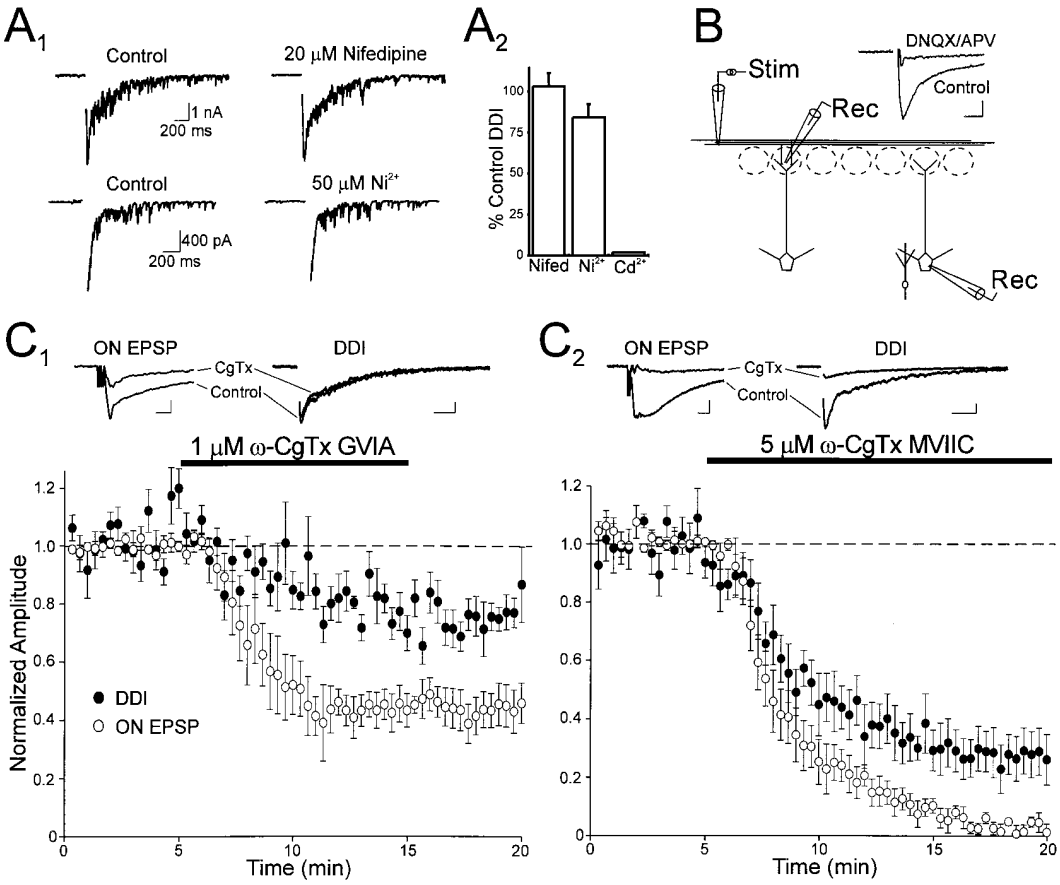

Figure 7. Calcium Channels Underlying Dendrodendritic Inhibition

(A_1) Individual records from different experiments showing that neither nifedipine (20 μM) nor nickel (50 μM) substantially reduce dendrodendritic inhibition.

(A_2) Summary of experiments using nifedipine or nickel. Application of cadmium (Cd^{2+}, 100 μM) completely blocks the response.

(B) Recording configuration for simultaneous measurements of dendrodendritic inhibition and olfactory nerve (ON) field EPSPs. Inset shows that the ON field EPSP recorded in the glomerulus of a slice is blocked by the application of APV (25 μM) and DNQX (20 μM). Scale bars, 0.2 mV and 10 ms.

(C_1) Summary plot of experiments examining the involvement of N-type calcium channels in dendrodendritic inhibition (closed circles) and excitatory transmission mediated by olfactory nerve fibers (open circles). The application of ω-conotoxin GVIA (1 μM) for the period marked by the bar caused a marked inhibition of the field EPSP, while the dendrodendritic response was less reduced. Upper sweeps are taken from a representative experiment, and the responses before (Control) and after application of ω-conotoxin GVIA (CgTx) are superimposed. Scale bars: 0.4 mV and 5 ms, field EPSPs; 1 nA and 200 ms, dendrodendritic inhibition (DDI).

(C_2) Summary plot of experiments examining the role of P/Q-type channels. The application of ω-conotoxin MVIIC (5 μM) for the period marked by the bar completely blocked the field EPSP and caused a dramatic reduction in the dendrodendritic response. Upper traces are taken from a typical experiment, and the responses before (Control) and after application of ω-conotoxin MVIIC (CgTx) are superimposed. Scale bars: 0.2 mV and 10 ms, field EPSPs; 1 nA and 200 ms, dendrodendritic inhibition (DDI). Experiments examining the actions of nifedipine and peptide toxins were performed in Mg^{2+}-free solution.

voltage step applied to Cell 1. The addition of APV blocked the self-inhibition of mitral Cell 1 and also abolished the lateral inhibition recorded in mitral Cell 2. Partial recovery of both responses followed washout of APV. The IPSCs mediating lateral inhibition reversed polarity at 0 mV and were blocked by BMI, indicating that they were $GABA_A$ receptor mediated (data not shown). Lateral inhibition has been found in ~10% of the mitral cell pairs examined (n = 40 pairs). These results demonstrate that glutamate release from mitral cell dendrites elicits GABAergic self-inhibition as well as lateral inhibition. In the absence of sodium-dependent action potentials, we conclude that lateral inhibition can be mediated by solely dendritic interactions between mitral and granule cells in the olfactory bulb.

Discussion

In this study, we have explored the mechanisms governing dendrodendritic inhibition in slices of the rat olfactory bulb. We found that NMDA receptors on granule cell spines play an important role in the generation of dendrodendritic inhibition. Back-propagating action potentials activate high threshold calcium channels that are tightly coupled to glutamate release sites in mitral cell dendrites. Our results also indicate that both N- and

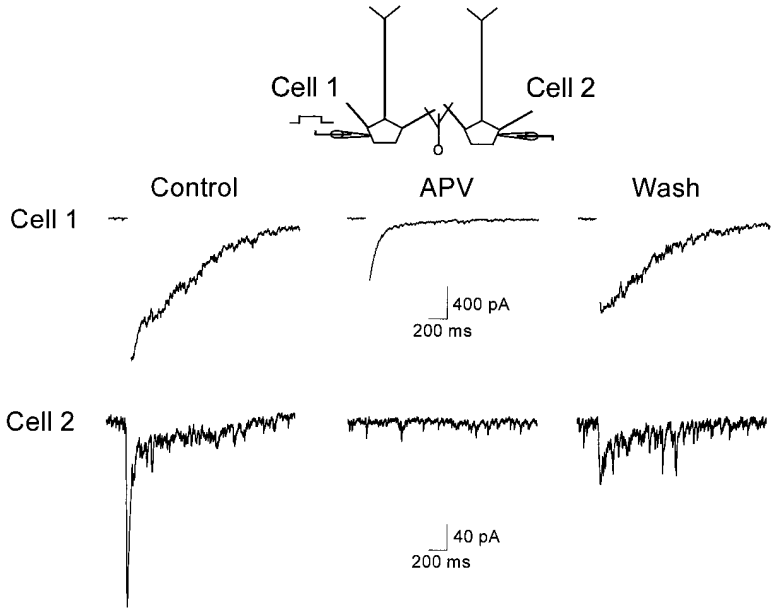

Figure 8. Lateral Inhibition Measured with Simultaneous Recordings from Two Mitral Cells in TTX (1 μM)

A voltage step is used to trigger dendrodendritic self-inhibition in Cell 1 (upper traces) while monitoring the response in a nearby (50 μm) unstimulated mitral cell (Cell 2, lower traces). Each trace represents the average of ~10 sweeps. The voltage step applied to Cell 1 causes a reliable IPSC in Cell 2. The subsequent addition of APV (25 μM) greatly reduces the dendrodendritic self-inhibition and blocks the lateral response recorded in Cell 2 (middle records). Both responses recover partially following washout of APV. Responses were recorded in Mg^{2+}-free solution.

P/Q-type calcium channels mediate dendritic transmission. We have also found that dendrodendritic transmission, independent of voltage-gated sodium channels, underlies lateral inhibition between mitral cells. These findings are summarized in Figure 9.

Role of NMDA Receptors in Dendrodendritic Inhibition

Previous studies of dendrodendritic inhibition in the turtle (Jahr and Nicoll, 1982b) and salamander (Wellis and Kauer, 1993) olfactory bulb demonstrated a role for glutamatergic transmission in triggering GABA release from granule cells. However, the identity of the excitatory receptors mediating this dendrodendritic response in the mammalian olfactory bulb remained unclear. In this study, we show that in low extracellular Mg^{2+}, dendrodendritic inhibition is mediated largely by glutamate acting on NMDA receptors present on granule cells, with little involvement of non-NMDA receptors. In the presence of physiological levels of Mg^{2+}, however, we observed dramatic reductions in dendrodendritic inhibition when either glutamate receptor subtype was blocked. Both NMDA and non-NMDA receptors have been suggested to contribute to feedback inhibition in salamander mitral cells (Wellis and Kauer, 1993). The simplest interpretation of our results is that non-NMDA receptors on granule cell spines provide the depolarization necessary to relieve the voltage-dependent Mg^{2+} block of NMDA receptors under physiological conditions. The very large enhancement of dendrodendritic inhibition we find when this block is reduced (in low Mg^{2+} Ringer's) suggests that NMDA receptors can preferentially activate this synaptic circuit.

The high calcium permeability of NMDA receptors raises the intriguing possibility that calcium influx through these receptors, rather than through voltage-activated calcium channels, initiates GABA release. We feel that this is unlikely since electron microscopic analysis (Price and Powell, 1970b) suggests that GABA release sites can be distant (~1 μm) from the postsynaptic densities in which the NMDA receptors are presumably concentrated. Synaptic transmitter release is generally considered to require very high local concentrations of calcium.

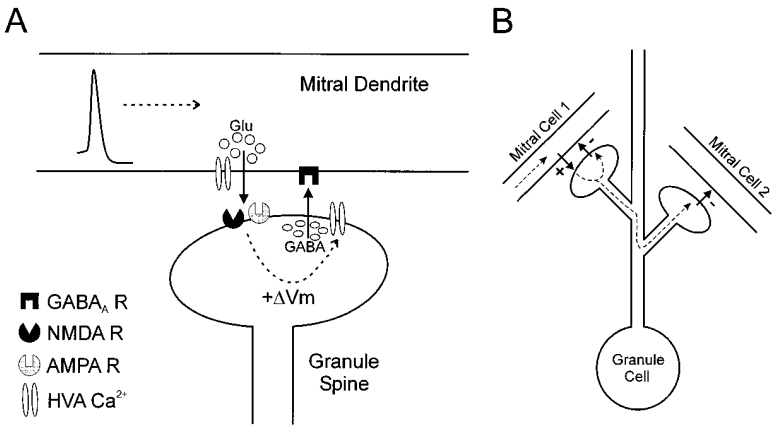

Figure 9. Summary Diagram Describing the Steps Governing Dendrodendritic Self-Inhibition and Lateral Inhibition

(A) Self-inhibition.

(B) Lateral inhibition. Dashed lines indicate the flow of excitation within mitral and granule dendrites.

Such calcium "microdomains" typically are generated by high threshold calcium channels in close proximity to transmitter release sites (Simon and Llinas, 1985; Adler et al., 1991; Dunlap et al., 1995; Mintz et al., 1995). The influx of calcium through distant NMDA receptors would be unlikely to provide the calcium concentrations required at the sites of GABA exocytosis. If GABA release is mediated instead by voltage-sensitive calcium channels (Figure 9A), either glutamate receptor subtype would be likely to depolarize the spine to threshold for calcium channel activation. Consistent with this hypothesis, while we find that NMDA receptors preferentially activate dendrodendritic responses, there is no absolute requirement for these receptors. Even in the presence of high concentrations of APV (100 μM), voltage steps still can evoke reciprocal dendrodendritic inhibition, which is blocked completely by DNQX (data not shown). Also as predicted by this model, we demonstrated (using focal depolarization) that voltage-gated calcium channels are coupled directly to GABA release in granule cell spines.

We have found that both NMDA and non-NMDA receptors mediate excitatory transmission from mitral to granule cells. This result is consistent with previous studies of EPSCs in salamander (Wellis and Kauer, 1994) and cultured rat olfactory bulb cells (Trombley and Westbrook, 1990). It is likely that both glutamate receptor subtypes are colocalized on granule cell spines, since we never observed evoked synaptic currents in granule cells mediated solely by NMDA receptors. Why, then, are NMDA receptors more effective at evoking GABA release than non-NMDA receptors? A major distinction between these two glutamate receptor types is the intrinsically slow kinetics of NMDA receptors (Lester et al., 1990). Modeling studies (Woolf et al., 1991; Koch and Zador, 1993) suggest that the faster, transient current through non-NMDA glutamate receptors will be greatly attenuated by the high impedance of spine necks. By contrast, the prolonged time course of the NMDA current is more likely to activate voltage-gated calcium channels governing GABA release in neighboring spines along the granule cell dendrite. In this way, NMDA receptors would be better suited than non-NMDA receptors to depolarize populations of granule spines to threshold for GABA release. This model implies that dendrodendritic transmission mediated solely by current through non-NMDA receptors would activate a relatively limited number of granule cell spines, whereas the current through NMDA receptors would recruit a much larger population of spines. In agreement with this model, we find that dendrodendritic responses evoked after blockade of NMDA receptors are greatly reduced in amplitude but still follow a time course similar to that seen under control conditions.

Dendrodendritic interactions are clearly not limited to the self-inhibition of mitral cells. We find strong evidence that dendritic synapses onto granule cells mediate lateral inhibition between mitral cells. Depolarization of a single mitral cell can lead to synchronous inhibition in that mitral cell as well as in neighboring mitral cells. Lateral interactions among mitral cells are likely mediated by the spread of a signal between granule cell spines (Figure 9B), since there is no anatomical evidence for the convergence of dendrites from multiple mitral cells onto single granule spines (see Price and Powell, 1970a, 1970b). It is unlikely that diffusion of calcium between spines is this signal, since spine necks appear to represent a significant barrier to calcium diffusion (Svoboda et al., 1996). As with NMDA-mediated self-inhibition and in accord with previous theoretical studies (Rall and Shepherd, 1968; Woolf et al., 1991), we believe that the signal mediating lateral inhibition is the spread of depolarization through granule cell dendrites.

Calcium Channels Governing Dendritic Transmission

Much attention has been focused on the relationship between calcium and transmitter release from conventional axonic nerve terminals. However, little is known about mechanisms governing transmitter release from presynaptic dendrites. Dendrites of central neurons express a variety of calcium channels, including T-, L-, N-, and P/Q-type (Westenbroek et al., 1990, 1992; Johnston et al., 1996), any of which may underlie transmitter release. The release of peptides from dendrites in the hippocampus has been suggested to rely on L-type calcium channels (Simmons et al., 1995). We find no evidence for the involvement of either T- or L-type channels in triggering glutamate or GABA release from dendrites in the olfactory bulb. Instead, similar to findings at conventional axonic synapses (Castillo et al., 1994; Dunlap et al., 1995; Mintz et al., 1995; Poncer et al., 1997), we find that N- and P/Q-type calcium channels govern the dendritic release of fast neurotransmitters in the olfactory bulb. Since dendrodendritic inhibition involves reciprocal synaptic transmission between mitral and granule cells, we cannot easily assign N and P/Q channels to specific synaptic locations. However, we have some evidence that these channels may be present at the mitral cell synapse, since calcium currents measured in our somatic recordings were reduced consistently by ω-conotoxins (data not shown). Additional experiments will be required to determine definitively the specific synaptic location of the calcium channels that underlie dendrodendritic inhibition.

An attractive feature of this olfactory circuit is the ability to measure and manipulate calcium dynamics in a large presynaptic structure, the mitral cell dendrite. Dendrodendritic inhibition recorded in a mitral cell can then be used as a detector of glutamate release from presynaptic mitral cell dendrites. Using this approach, the complete blockade of dendrodendritic inhibition in BAPTA-loaded mitral cells confirms the central role of calcium in dendritic transmitter release. The greater sensitivity of dendrodendritic inhibition to BAPTA versus EGTA suggests that, as with axonic terminals, the sites of calcium entry must be close to the exocytotic machinery in mitral cell dendrites (Adler et al., 1991). The partial reduction of dendrodendritic responses in EGTA-loaded mitral cells may reflect some contribution of calcium channels that are relatively distant from glutamate release sites (Borst and Sakmann, 1996; Salin et al., 1996). Alternatively, the slow buffering kinetics of EGTA may suffice when used at very high concentrations.

We have also used simultaneous measurements of

dendrodendritic inhibition and calcium influx to explore further the relationship between calcium and dendritic glutamate release. By varying the amplitude of voltage steps applied to mitral cells, we found a close correspondence between dendritic calcium influx and dendrodendritic inhibition in Mg^{2+}-free solution. Given that our measurements reflect output from two coupled synapses, we cannot determine directly the transfer function that relates dendritic calcium influx to glutamate release. Nevertheless, we can infer some aspects of the input/output relationship of this reciprocal network. The high threshold of both dendrodendritic inhibition and calcium influx into mitral cell dendrites suggests that only action potentials in mitral cells trigger dendrodendritic inhibition in vivo. Indeed, we consistently observe that mitral cell dendrites support the back-propagation of large-amplitude action potentials, in accordance with several recent studies (Bischofberger and Jonas, 1997; Chen et al., 1997). In neocortical pyramidal neurons, calcium accumulation can be linearly related to action potential frequency (Helmchen et al., 1996). The parallel relationship we found between calcium influx and dendrodendritic inhibition raises the possibility that dendrodendritic inhibition can be linearly related to the frequency of mitral cell action potentials.

The time course of dendrodendritic inhibition is remarkably slow. Yet, dendrodendritic inhibition is clearly composed of the summation of many unitary GABAergic IPSCs with rapid kinetics, similar to those seen elsewhere in the brain (Galarreta and Hestrin, 1997). Our results suggest that calcium clearance from mitral cell dendrites occurs too rapidly to be the rate-limiting step in dendrodendritic inhibition. Dendrodendritic responses are also significantly slower than NMDA receptor–mediated EPSCs (Lester et al., 1990), suggesting that NMDA receptor kinetics alone cannot account for the slow time course of these responses. One possibility we have not yet explored is that GABA release from granule cells is prolonged due to the intrinsic properties of these cells. Regenerative calcium potentials in granule cell dendrites could provide a long-lasting stimulus for GABA release.

Experimental Procedures

Horizontal slices (300–400 μm) of the olfactory bulb were prepared from 14- to 35-day-old Sprague-Dawley rats using conventional methods (Isaacson and Walmsley, 1995) and viewed under DIC optics (Axioskop FS, Carl Zeiss). The slices were superfused with a Ringer's solution containing (in mM): 119 NaCl, 5 KCl, 1.3 Mg_2SO_4, 2.5 $CaCl_2$, 1 NaH_2PO_4, 26.2 $NaHCO_3$, and 11 glucose that was equilibrated with 95% O_2, 5% CO_2. As indicated in the figure legends, some experiments were performed using the same superfusing solution but without the addition of Mg^{2+}. In experiments using peptide toxins, the superfusing solution was supplemented with nifedipine or nitrendipine (10 μM) and cytochrome C (1 mg/ml). Except where noted, all experiments were performed in the presence of tetrodotoxin (TTX, 1 μM). At this concentration, TTX abolished fast Na^+ current in voltage-clamp recordings and olfactory nerve-evoked synaptic responses (data not shown). In most experiments examining the actions of DNQX, glycine (10–20 μM) was added to the superfusing solution. Patch electrodes (1.5–3 MΩ resistance) for voltage-clamp recordings contained (in mM): 120 CsCl, 10 TEA-Cl, 20 HEPES, 12 phosphocreatine, 3 MgATP, 0.2 Na_3GTP, and 0.2 EGTA (pH 7.3). For current-clamp recordings, the internal solution was identical except that 135 mM $KMeSO_4$ was substituted for the CsCl and TEA-Cl. Series resistance, which was <10 MΩ, was routinely compensated by >80%. Unless indicated otherwise, the holding potential was −70 mV and experiments were performed primarily at room temperature (22°C–25°C). Some pharmacological experiments were performed at 30°C. The temperature sensitivity (Q_{10}) of dendrodendritic inhibition was determined in individual cells by varying the temperature of the superfusing solution.

Fluorescent calcium transients were measured using a photodiode and a high gain current-to-voltage converter (5 GΩ feedback resistor). Mitral cells were loaded with a calcium-sensitive indicator dye (either Oregon Green or Oregon Green-5N, Molecular Probes) through the whole-cell pipette and illuminated using a 150 W Xe lamp (Opti-Quip) and a 485 nm excitation filter. Emitted fluorescence was detected using a 505 nm dichroic mirror and a 530 nm barrier filter (Omega Optical). An area of interest was defined by restricting the illumination to a spot ~50 μm in diameter that was positioned along the dendrite or soma of a filled mitral cell. Data is reported as fractional changes (ΔF/F) of the photodiode output. The low affinity calcium dye, Oregon Green-5N, was used in voltage-clamp experiments to reduce signal artifacts due to dye saturation. In these recordings, the indicator dye clearly was not saturated by the calcium influx during short steps used to evoke dendrodendritic inhibition, since longer duration steps elicited significantly larger fluorescent transients (data not shown).

Field EPSPs were evoked via a Ringer's-filled pipette (tip diameter 10–20 μm) placed within the olfactory nerve layer. Extracellular recordings were made from similar pipettes placed within individual glomeruli. Field EPSPs were recorded with an Axoclamp-2B (Axon Instruments), filtered at 1 kHz, and digitized at 5 kHz. Dual somatic and dendritic recordings were obtained using the two headstages of an Axoclamp-2B in bridge mode. Smaller patch pipettes were used for dendritic recordings (5–7 MΩ). Action potentials were filtered at 5 kHz and sampled at 50 kHz. Dendritic recording locations relative to the soma were measured from a video DIC image of the cell using an image processor (Argus-10, Hamamatsu). Synaptic currents were recorded with an Axopatch-1D amplifier (Axon Instruments). Currents were filtered at 2 kHz before being digitized at 5 or 10 kHz. Data were analyzed with pClamp (Axon Instruments) and custom-written software. Dendrodendritic inhibition was quantified by calculating the current integral over a 2 s period beginning 50–100 ms after the end of the voltage step. In some figures, synaptic currents represent the average of 5–10 sweeps. Action potential amplitude was measured from the resting membrane potential. Data are shown as mean ± SEM.

Acknowledgments

We thank Dr. Kerry Delaney for helpful discussions. We are grateful to Drs. Albert Berger and Bertil Hille for support and helpful comments on the manuscript. This study was supported by a Burroughs Wellcome Fund Career Award in Biomedical Science (to J. S. I.) and by the National Institutes of Health (NS33590 to B. W. S.).

Received December 9, 1997; revised January 4, 1998.

References

Adler, E.M., Augustine, G.J., Duffy, S.N., and Charlton, M.P. (1991). Alien intracellular calcium chelators attenuate neurotransmitter release at the squid giant synapse. J. Neurosci. *11*, 1496–1507.

Aroniodou-Anderjaska, V., Ennis, M., and Shipley, M.T. (1997). Glomerular synaptic responses to olfactory nerve input in rat olfactory bulb slices. Neuroscience *79*, 425–434.

Avery, R.B., and Johnston, D. (1996). Multiple channel types contribute to the low-voltage–activated calcium current in hippocampal CA3 pyramidal neurons. J. Neurosci. *16*, 5567–5582.

Bischofberger, J., and Jonas, P. (1997). Action potential propagation into the presynaptic dendrites of rat mitral cells. J. Physiol. *504*, 359–365.

Borst, J.G., and Sakmann, B. (1996). Calcium influx and transmitter release in a fast CNS synapse. Nature *383*, 431–434.

Brennan, P.A., and Keverne, E.B. (1997). Neural mechanisms of mammalian olfactory learning. Prog. Neurobiol. *51*, 457–481.

Castillo, P.E., Weisskopf, M.G., and Nicoll, R.A. (1994). The role of Ca^{2+} channels in hippocampal mossy fiber synaptic transmission and long-term potentiation. Neuron *12*, 261–269.

Chen, W.R., Midtgaard, J., and Shepherd, G.M. (1997). Forward and backward propagation of dendritic impulses and their synaptic control in mitral cells. Science *268*, 463–467.

Cheramy, A., Leviel, V., and Glowinski, J. (1981). Dendritic release of dopamine in the substania nigra. Nature *289*, 537–542.

Collingridge, G.L., and Lester, R.A.J. (1989). Excitatory amino acid receptors in the vertebrate central nervous system. Pharmacol. Rev. *40*, 143–210.

Cotman, C.W., and Iverson, L.L. (1987). Excitatory amino acids in the brain—focus on NMDA receptors. Trends Neurosci. *7*, 263–265.

Dowling, J.E. (1968). Synaptic organization of the frog retina: an electron microscopic analysis comparing the retinas of frogs and primates. Proc. R. Soc. Lond. [Biol.] *170*, 205–228.

Dunlap, K., Luebke, J.I., and Turner, T.J. (1995). Exocytotic Ca^{2+} channels in mammalian central neurons. Trends Neurosci. *18*, 89–98.

Galarreta, M., and Hestrin, S. (1997). Properties of $GABA_A$ receptors underlying inhibitory synaptic currents in neocortical pyramidal neurons. J. Neurosci. *17*, 7220–7227.

Helmchen, F., Imoto, K., and Sakman, B. (1996). Ca^{2+} buffering and action potential–evoked Ca^{2+} signaling in dendrites of pyramidal neurons. Biophys. J. *70*, 1069–1081.

Isaacson, J.S., and Walmsley, B. (1995). Receptors underlying excitatory synaptic transmission in slices of the rat anteroventral cochlear nucleus. J. Neurophysiol. *73*, 964–973.

Jahr, C.E., and Nicoll, R.A. (1980). Dendrodendritic inhibition: demonstration with intracellular recording. Science *207*, 1473–1475.

Jahr, C.E., and Nicoll, R.A. (1982a). An intracellular analysis of dendrodendritic inhibition in the turtle in vitro olfactory bulb. J. Physiol. *326*, 213–234.

Jahr, C.E., and Nicoll, R.A. (1982b). Noradrenergic modulation of dendrodendritic inhibition in the olfactory bulb. Nature *297*, 227–229.

Johnston, D., Magee, J.C., Colbert, C.M., and Christie, B.R. (1996). Active properties of neuronal dendrites. Annu. Rev. Neurosci. *19*, 165–186.

Koch, C., and Zador, A. (1993). The function of dendritic spines: devices subserving biochemical rather than electrical compartmentation. J. Neurosci. *13*, 413–422.

Lester, R.J., Clements, J.D., Westbrook, G.L., and Jahr, C. (1990). Channel kinetics determine the time course of NMDA receptor–mediated synaptic currents. Nature *346*, 565–567.

Magee, J.C., and Johnston, D. (1995). Characterization of single voltage-gated Na^+ and Ca^{2+} channels in apical dendrites of rat CA1 pyramidal neurons. J. Physiol. *481*, 67–90.

Mintz, I.M., Sabatini, B.L., and Regehr, W.G. (1995). Calcium control of transmitter release at a cerebellar synapse. Neuron *15*, 675–688.

Nicoll, R.A. (1969). Inhibitory mechanisms in the rabbit olfactory bulb: dendrodendritic mechanisms. Brain Res. *14*, 157–172.

Nowycky, M.C., Mori, K., and Shepherd, G.M. (1981). GABAergic mechanisms of dendrodendritic synapses in isolated turtle olfactory bulb. J. Neurophysiol. *46*, 639–648.

Phillips, C.G., Powell, T.P.S., and Shepherd, G.M. (1963). Responses of mitral cells to stimulation of the lateral olfactory tract in the rabbit. J. Physiol. *168*, 65–88.

Poncer, J.C., McKinney, R.A., Gahwiler, B.H., and Thompson, S.M. (1997). Either N- or P-type calcium channels mediate GABA release at distinct hippocampal inhibitory synapses. Neuron *18*, 463–472.

Price, J.L., and Powell, T.P.S. (1970a). The morphology of the granule cells of the olfactory bulb. J. Cell Sci. *7*, 91–123.

Price, J.L., and Powell, T.P.S. (1970b). The synaptology of the granule cells of the olfactory bulb. J. Cell Sci. *7*, 125–155.

Rall, W., and Shepherd, G.M. (1968). Theoretical reconstruction of field potential and dendrodendritic synaptic interactions in olfactory bulb. J. Neurophysiol. *31*, 884–915.

Rall, W., Shepherd, G.M., Reese, T.S., and Brightman, M.W. (1966). Dendrodendritic synaptic pathway for inhibition in the olfactory bulb. Exp. Neurol. *14*, 44–56.

Randall, A., and Tsien, R.W. (1997). Contrasting biophysical and pharmacological properties of T-type and R-type calcium channels. Neuropharmacology *36*, 879–893.

Salin, P.A., Scanziani, M., Malenka, R.C., and Nicoll, R.A. (1996). Distinct short-term plasticity at two excitatory synapses in the hippocampus. Proc. Natl. Acad. Sci. USA *93*, 13304–13309.

Shepherd, G.M., and Greer, C.A. (1990). Olfactory bulb. In The Synaptic Organization of the Brain (New York: Oxford University Press), pp. 133–169.

Simmons, M.L., Terman, G.W., Gibbs, S.M., and Chavkin, C. (1995). L-type calcium channels mediate dynorphin neuropeptide release from dendrites but not axons of hippocampal granule cells. Neuron *14*, 1265–1272.

Simon, S.M., and Llinas, R.R. (1985). Compartmentalization of the submembrane calcium activity during calcium influx and its significance in transmitter release. Biophys. J. *48*, 485–498.

Stuart, G., Spruston, N., Sakmann, B., and Häusser, M. (1997). Action potential initiation and backpropagation in neurons of the mammalian CNS. Trends Neurosci. *20*, 125–131.

Svoboda, K., Tank, D.W., and Denk, W. (1996). Direct measurement of coupling between dendritic spines and shafts. Science *272*, 716–719.

Takahashi, T., and Momiyama, A. (1993). Different types of calcium channels mediate central synaptic transmission. Nature *366*, 156–158.

Trombley, P.Q., and Westbrook, G.L. (1990). Excitatory synaptic transmission in cultures of rat olfactory bulb. J. Neurophys. *64*, 598–606.

von Gersdorff, H., and Matthews, G. (1994). Dynamics of synaptic vesicle fusion and membrane retrieval in synaptic terminals. Nature *367*, 735–739.

Wellis, D.P., and Kauer, J.S. (1993). $GABA_A$ and glutamate receptor involvement in dendrodendritic synaptic interactions from salamander olfactory bulb. J. Physiol. *469*, 315–339.

Wellis, D.P., and Kauer, J.S. (1994). GABAergic and glutamatergic synaptic input to identified granule cells in salamader olfactory bulb. J. Physiol. *475*, 419–430.

Westenbroek, R.E., Ahlijanian, M.K., and Catterall, W.A. (1990). Clustering of L-type Ca^{2+} channels at the base of major dendrites in hippocampal pyramidal neurons. Nature *347*, 281–284.

Westenbroek, R.E., Hell, J.W., Warner, C., Dubel, S.J., Snutch, T.P., and Catterall, W.A. (1992). Biochemical properties and subcellular distribution of an N-type calcium channel $\alpha 1$ subunit. Neuron *9*, 1099–1115.

Wheeler, D.B., Randall, A., and Tsien, R.W. (1994). Roles of N-type and Q-type Ca^{2+} channels in supporting hippocampal synaptic transmission. Science *264*, 107–111.

Winslow, J.L., Duffy, S.N., and Charlton, M.P. (1994). Homosynaptic facilitation of transmitter release in crayfish is not affected by mobile calcium chelators: implications for the residual ionized calcium hypothesis from electrophysiological and computation analyses. J. Neurophysiol. *72*, 1769–1793.

Woolf, T.B., Shepherd, G.M., and Greer, C.A. (1991). Local information processing in dendritic trees: subsets of spines in granule cells of the mammalian olfactory bulb. J. Neurosci. *11*, 1837–1854.

Yokoi, M., Mori, K., and Nakanishi, S. (1995). Refinement of odor molecule tuning by dendrodendritic synaptic inhibition in the olfactory bulb. Proc. Natl. Acad. Sci. USA *92*, 3371–3375.